



Article

Energy Performance Analysis of the Renovation Process in an Italian Cultural Heritage Building

Nikolaos Ziozas ¹, Angeliki Kitsopoulou ¹, Evangelos Bellos ¹, Petros Iliadis ¹, Dimitra Gonidaki ¹, Komninos Angelakoglou ¹, Nikolaos Nikolopoulos ¹, Silvia Ricciuti ² and Diego Viesi ^{2,*}

¹ Centre for Research and Technology Hellas (CERTH), Chemical Process and Energy Resources Institute (CPERI), Aigialeias 52, 15125 Marousi, Greece; n.ziozas@certh.gr (N.Z.); a.kitsopoulou@certh.gr (A.K.); e.belllos@certh.gr (E.B.); iliadis@certh.gr (P.I.); d.gonidaki@certh.gr (D.G.); angelakoglou@certh.gr (K.A.); n.nikolopoulos@certh.gr (N.N.)

² Fondazione Bruno Kessler (FBK), Center for Sustainable Energy (SE), Via Sommarive 18, 38123 Povo, TN, Italy; sricciuti@fbk.eu

* Correspondence: viesi@fbk.eu

Abstract: Renovating buildings with cultural heritage significance is an important step toward achieving sustainability in our cities. The benefits are not only energy-related but also encompass social aspects that make these renovations a high priority. The present work investigates the renovation process of a cultural heritage building in the Municipality of Trento in Italy, specifically focusing on achieving energy savings and renewable energy integration by implementing various renovation actions. These renovation actions include improvements to the building envelope, such as roof insulation and window replacements. Additionally, the renovation actions for active systems involve the installation of a ground-source heat pump for heating/cooling coupled with a borehole thermal energy storage system, which is an innovative technology for the renovation of cultural heritage buildings. The electrical systems of the building are upgraded through the addition of standard rooftop photovoltaics, innovative building-integrated photovoltaics (shingles), and the installation of an LED lighting system. The baseline and the renovation scenarios are studied using the dynamic simulation tool INTEMA.building, written in the programming language Modelica. This tool simulates both the building envelope and the energy systems with a high level of detail, using advanced control systems and adjustable time steps. According to the simulation analysis, the primary energy demand is reduced by 30.49%, the final energy demand by 36.74%, and the net electricity demand by 8.72%. Results from this study can be useful to interested stakeholders (e.g., building owners, architects, construction companies, public agents, and urban planners) dealing with the renovation of cultural heritage and protected buildings. Also, the results can be exploited for estimating energy savings by applying advanced renovation strategies for cultural heritage buildings.



Citation: Ziozas, N.; Kitsopoulou, A.; Bellos, E.; Iliadis, P.; Gonidaki, D.; Angelakoglou, K.; Nikolopoulos, N.; Ricciuti, S.; Viesi, D. Energy Performance Analysis of the Renovation Process in an Italian Cultural Heritage Building. *Sustainability* **2024**, *16*, 2784. <https://doi.org/10.3390/su16072784>

Academic Editors: Reza Daneshzarian, Elena Lucchi, Tianyi Chen and Wen Zhang

Received: 30 January 2024

Revised: 7 March 2024

Accepted: 21 March 2024

Published: 27 March 2024



Copyright: © 2024 by the authors. Licensee MDPI, Basel, Switzerland. This article is an open access article distributed under the terms and conditions of the Creative Commons Attribution (CC BY) license (<https://creativecommons.org/licenses/by/4.0/>).

1. Introduction

The decarbonization of the incumbent worldwide energy regime due to the climate crisis's escalation over the last decade highlights the contribution of the building sector to the associated total energy consumption and greenhouse gas emissions as well [1]. Characteristically, the building sector is responsible for approximately 15% of the world's total CO₂ emissions and about one-third of the total global final energy consumption [2]. Respectively, buildings account for 40% of the total energy consumption in the European Union and 36% of energy-related greenhouse gas emissions [3]. For that reason, the European Union has set building decarbonization at the forefront of its energy policy agenda, acknowledging energy efficiency measures as a core pillar towards a net-zero buildings pathway [4]. Under the energy efficiency obligation's schemes, European Union member countries should follow an average annual energy savings rate of 1.49% from 2024

to 2030 and an annual renovation rate of 3% for their public buildings [3]. Additionally, the integration of renewable energy sources, as well as the commercialization of high-technology solar energy systems would positively contribute to the decarbonization of energy systems for the future of the European community [5].

However, the outdated stock of the European Union's buildings challenges the commitment to energy efficiency directives, as over 60% of European buildings were built before 1980 [6]. Over 70% of the building stock is aged in the southern European countries (i.e., Italy, Greece, Spain, Cyprus, etc.) [6]. This status quo indicates the need for applied energy retrofitting interventions to enhance the poor energy performance of these buildings due to their outdated energy systems, structural elements, and materials [7]. Nonetheless, over 25% of these European aged buildings constitute historical or so-called cultural heritage buildings, challenging the integration of energy-efficient interventions [8].

Therefore, it is crucial to investigate proper sustainable technologies and retrofitting interventions to improve their energy performance without compromising their cultural and social idiosyncrasies [9].

1.1. Literature Review

Typical energy renovation interventions for historical buildings concern the insulation of roofs and walls, the installation of renewable energy technologies (i.e., solar panels, geothermal pumps, etc.), the integration of upgraded heating, ventilation, and air conditioning (HVAC) systems and respective control systems, and the replacement of lighting and electrical equipment [10]. Nevertheless, the unique feature of historical buildings' renovation is the accomplishment of tradeoffs between energy-efficient/renewable interventions and the preservation of their cultural and historical heritage. Arumägi et al. [11] implemented a renovation strategy consisting of insulation and HVAC interventions in a historical wooden apartment, resulting in a primary energy reduction of up to 65% and economic energy savings of up to 50%. Ardente et al. [12] found that building envelope enhancement was the most energy-efficient measure in their retrofit of six historical buildings. Another interesting retrofitting intervention implemented by Fonseca et al. [13] concerned the integration of an intelligent lighting system in public schools, while Cohen et al. [14] proposed that ceiling and wall insulation are more cost-effective than the replacement of windows for an energy consumption metering system during the retrofit of a single-family building. The installation of ground-source heat pumps (GSHPs) was studied by Boait et al. [15] as an energy-efficient action in retrofitting historical buildings in the United Kingdom. Their results show the heat pumps' poor seasonal performance compared to similar European studies, emphasizing the importance of the building's thermal behavior and characteristics. Hens [16] concluded that enriching the building envelope and ventilation system performs better in terms of energy savings than the installation of solar boilers and PV panels in a retrofit of a historical building built in 1957.

Gravagnuolo et al. [17] approached the retrofit of four historic buildings in Salerno from a transdisciplinary viewpoint by developing a multicriteria decision-making framework to evaluate the examined renovation solutions. This innovative approach led to the co-production of knowledge among designers, stakeholders, and citizens, resulting in a democratic decision-making process and respecting the cultural heritage of the community as a whole. De Toro et al. [18] focus on evaluating design-supporting tools, such as geographic information systems, for the restoration of cultural heritage buildings. At the same time, the Green Building Council protocol in Italy proposes an evaluation process for such buildings, including their cultural status and life-cycle analysis during the retrofit intervention phase [17].

However, implementing the above energy-efficient/renewable measures requires extensive energy and architectural analyses of historical buildings through energy modeling and simulation tools, as the majority of these buildings were built from local resources and materials lacking detailed drawings and studies [19]. For example, Ascione et al. [20] model and simulate a historical building in Benevento, Italy using EnergyPlus software

(Version 7.0), providing viable energy retrofit solutions. Similarly, Harrestrup and Svendsen [21] evaluate the energy behavior of a multi-story brick building in Copenhagen by simulating the integration of exterior wall insulation before and after the renovation. Sahin et al. [22] ran simulations for a 19th-century educational center in Turkey, comparing passive and active energy-efficient measures. They conclude that energy savings of up to 34% can be reached without compromising the building's heritage value. On the other hand, Moran et al. [8] performed steady-state calculations using the Passive House Planning Package version 7.0 software for Georgian dwellings in Bath, the United Kingdom, questioning the accuracy of the occupants' thermal comfort with the associated tested heating patterns. Likewise, Zagorskas et al. [23] point out the mismatch of energy simulation software for historical buildings between actual and simulated thermal performances due to the lack of modeling accuracy for the building envelope. From another perspective, Serano et al. [24] implemented a life-cycle assessment of a historical building in Denmark, comparing the most suitable option between a restoration scenario and a renovation scenario. Their research concludes that the restoration scenario performs slightly better in terms of both energy savings and architectural style [24].

1.2. Research Contribution

The previous survey of the literature indicates a great interest in the renovation of buildings with cultural heritage importance due to the numerous energy- and society-related benefits. In this direction, the present work examines a deep renovation strategy of a building with cultural heritage status located in Trento, Italy [25]. The examined location is of great importance as the province of Trento possesses 700 public heritage buildings, of which 166 belong to the public building stock with a registered consumption higher than 45 kWh/m³y [26]. Moreover, the geographical location of this retrofit scenario raises scientific interest, as the research on Italian historical buildings is considered to be the most active of its kind worldwide [9]. This can be attributed to the fact that 31% of Italy's total structures were constructed before 1945, and approximately 12% were constructed before 1919 [27]. This work's novelty lies in its use of an innovative, dynamic simulation tool that allows a thorough investigation of suitable energy-efficient/renewable solutions in a building with a substantial floor area (about 5400 m²). Specifically, an analysis is conducted using the INTEMA.building tool, a simulation tool developed in the Modelica programming language [28], using the Dymola interface [29]. This tool presents numerous advancements because it precisely models the control systems of a building, provides detailed simulations of both the building envelope and the energy systems, and effectively solves problems with high accuracy due to the adjustable time step of the solving procedure. Also, the value of this work lies in it being based on the renovation of a cultural heritage building with some special characteristics like a high floor area and geometrical/space limitations regarding the installation of new renovation technologies. Furthermore, the most critical limitation of this research is the conservation of the building's historical idiosyncrasies and architectural features throughout the renovation process. Another novel aspect lies in the incorporation of an innovative ground-source heat pump in the renovation, as the majority of the incumbent renovations in cultural heritage buildings are based mostly on the application of technologies like solar thermal collectors and photovoltaics [30]. The results of this work indicate the energy-related benefits of the renovation process and can serve as a guideline for future renovations in cultural heritage buildings, especially for buildings with special characteristics like the studied building.

2. Materials and Methods

This section includes a basic description of the studied building's baseline and renovation scenarios. The data for the building envelope and the energy systems are given, and the simulation strategy is clearly described.

2.1. The Studied Building—Baseline Scenario

The examined building, located and managed by the Municipality of Trento (Italy), is a cultural heritage building that serves as a pivotal center of cultural and recreational activities in the city. This building's use has changed several times over the centuries: it went from being a monastery (1235–1810) to being a hospital (1810–1970) to being a university (1970–2018) until its current use as one of the most important centers of cultural and recreational activities in the city. Specifically, the building is located in the Santa Chiara District of Trento, with a latitude of 46.063281° and a longitude of 11.124574° , with a 10° counter-clockwise deviation from the direction of north. It is partially adjacent to a gym and an auditorium on the east side and to a church on the west side. Figure 1 depicts both the entrance of the examined building and a top view of the building retrieved from a satellite photograph from Google Earth, showcasing the azimuth angles of its external walls. The design drawings and construction plans of the building, including a top view and three different cross sections, are demonstrated in Figure 2.



Figure 1. Photograph of the examined building before the renovation: (a) entrance; (b) depiction from a satellite image with azimuth orientation angles.

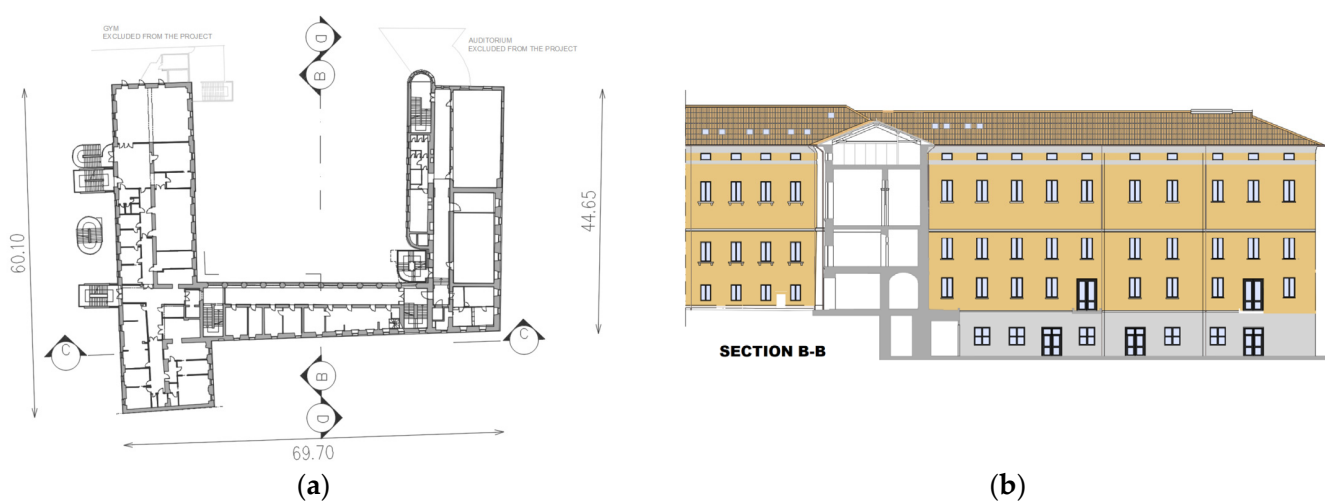


Figure 2. Cont.

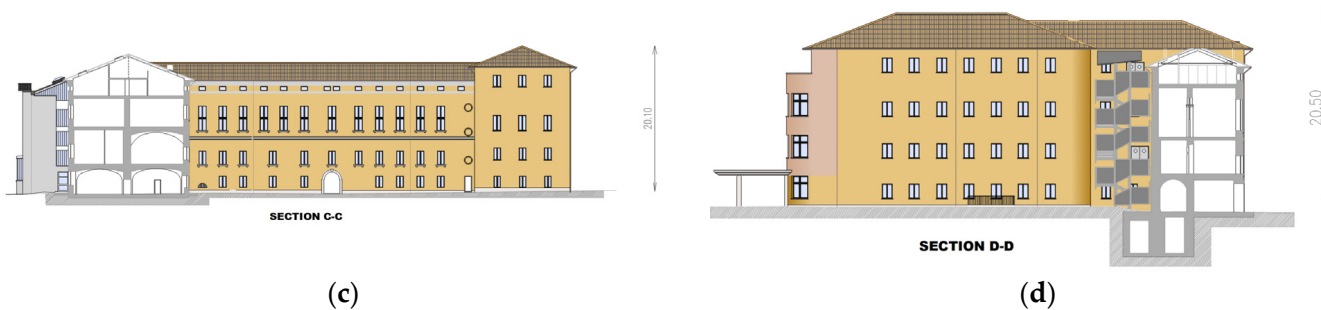


Figure 2. Drawings of the examined building before the renovation: (a) top view with basic dimensions; (b) B-B cross section, (c) C-C cross section, (d) D-D cross section.

2.1.1. Building Envelope Description

The building consists of five floors and a partially heated basement, with a mean total height of 20.3 m, while the mean internal height of each floor equals 3 m. Additionally, the building's conditioned floor area is calculated at 5400 m², 17% of which serves as a guesthouse. The thermal envelope of the building consists of the part of the basement that is heated, the ground floor, and four additional floors above. The basement's ground slab is in contact with the ground and has a nominal U-value of 2.2 W/m²K, whereas the basement's ceiling is characterized by a nominal U-value of 1.8 W/m²K. The ground floor is in contact with the basement and the two are separated by the basement ceiling. The external and basement walls are denoted by a U-value of 0.7 W/m²K, while the roof construction's total thermal transmittance value is estimated at 0.5 W/m²K. The building's glazing system consists of double-pane windows with a total U-value of 2.5 W/m²K, including the glazing, frame, and thermal bridge effects. The absorbance of the opaque structural elements was estimated at 60% and the emittance was estimated at 80%, which are typical values according to [31]. Regarding the windows, the emittance value is estimated at 90% and the g-value is estimated to be 84%. Table 1 includes basic information regarding the detailed description of the examined building envelope.

Table 1. Basic data for the description of the examined building's envelope.

Parameter	Value
Opaque structural elements	
U-value of the external walls (W/m ² K)	0.70
U-value of the roof (W/m ² K)	0.50
U-value of the basement ceiling (W/m ² K)	1.80
U-value of the ground slab (W/m ² K)	2.20
Slope of the roof (°)	22
Absorbance (%)	60
Emittance (%)	80
Slope of the roof (°)	22
Transparent structural elements	
U-value of the window (W/m ² K)	2.5
g-value of the window	0.84
Emittance (%)	80

Table 2 gives the areas of the building's structural components for every orientation and the adjacency of the building's external walls. Specifically, the external walls are in contact with either ambient air, a neighboring building, or the ground. The sum of these three cases gives the total area of the external walls for each orientation. It is mentioned that the present building has windows in all directions, with the largest opening areas being located on the east- and south-oriented façades.

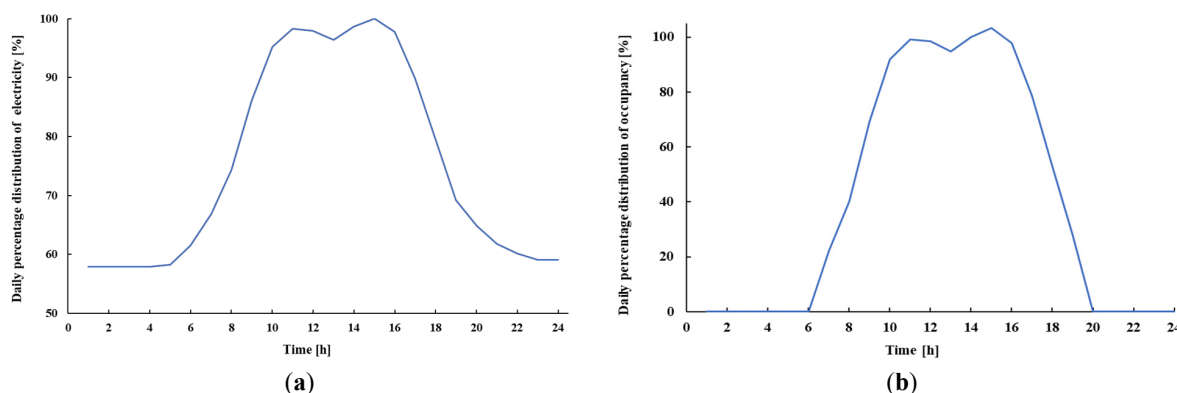
Table 2. Geometrical calculations of the external walls, roofs, and windows.

Summary Table of Areas [m ²]						
	Roofs	Windows	External Walls	External Walls in Contact with:		
Orientation	Total Area	Total Area	Total Area	Ambient Air	Neighboring Building	Ground
North ($\gamma = -10^\circ$)	1157	134	1916	1695	0	221
South ($\gamma = 170^\circ$)	1122	215	1704	1388	95	221
East ($\gamma = -100^\circ$)	521	182	1145	907	135	103

Table 3 includes operational parameters correlated with the building's internal loads and aeration loads. The specific loads are given per conditioned area, equal to 5400 m². Additionally, the mean operating factors were estimated according to the usual occupancy of the building. Specifically, the daily operating profile of the building follows the profile illustrated in Figure 3a, which corresponds to the percentage of the maximum electricity load throughout a typical day [32]. Regarding the building's occupancy profile, its maximum occupancy is 200 occupants, while Figure 3b illustrates the daily distribution of the occupancy. The infiltration and natural ventilation rates are selected to be 0.35 and 0.7 air changes per hour (ACH), respectively.

Table 3. Operating parameters of the examined building for the baseline scenario.

Parameter	Value
Mean daily occupants	200
Thermal load of the occupants (W/person)	80
Mean operating fraction of the occupants (%)	30
Specific electrical load of the lighting (W/m ²)	9
Mean operating fraction of the lighting (%)	40
Specific electrical load of the appliances (W/m ²)	4
Mean operating fraction of the appliances (%)	50
Infiltration rate (ACH)	0.35
Natural ventilation rate (ACH)	0.7

**Figure 3.** Daily distribution of (a) the electrical energy consumption and (b) the occupancy of the building [32].

2.1.2. Energy System Description

The space heating system of the building includes radiators, which are distributed throughout the entire building and are fed by hot water. The hot water is produced by two efficient condensing gas boilers with a nominal efficiency of 98.2% and a capacity of 534 kW and 584 kW. The distribution thermal losses are estimated to be 15% due to the relatively high distance between the gas boilers and the radiators. For the heating period, which in adherence to Italian regulations begins on the 14th of October and ends on the

16th of April, the air temperature setpoint is configured at 20 °C. The space cooling system of the building includes several air-to-air heat pumps (split units) of various capacities. The nominal efficiency of the heat pumps is estimated to be EER = 2.16. The temperature setpoint for the cooling period is set to 26 °C, whereas no specific regulations determine the time period of the cooling season. Indicatively, the need for cooling exists from the middle of May up to the end of September. For the purposes of the energy analysis and because a single heating-and-cooling system serves the entire building under the same temperature setpoints, the building is considered a single thermal zone [31].

The DHW is produced by local electrical heaters, which are located in the building's bathrooms. The DHW temperature setpoint is 48 °C, and the occupants' mean daily demand is approximately 22 L per person. A typical profile representing the daily hot water demand distribution is shown in Figure 4, which considers a variable demand distribution throughout the day that keeps up with the occupancy profile of the building. The tap water coming from the network has an annual mean temperature of around 12 °C, and a typical water temperature variation during the year was selected [33]. Electrical heaters cover the DHW demand with an efficiency of 90%, including distribution losses. Table 4 summarizes the energy system's parameters regarding the space heating and cooling and the DHW production for the baseline scenario.

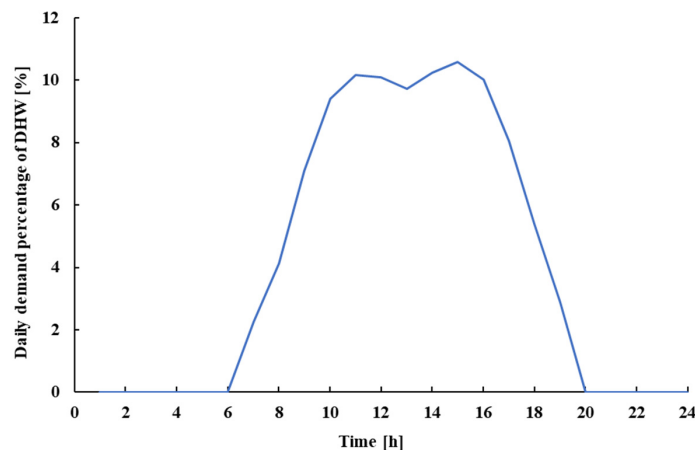


Figure 4. Daily dimensionless distribution of the hot water quantity demand.

Table 4. Energy system parameters for space heating and cooling and DHW production in the baseline scenario.

Parameter	Value
Heating system (condensing gas boiler)	
Temperature setpoint (°C)	20
Nominal capacity of the first condensing gas boiler (kW)	534
Nominal capacity of the second condensing gas boiler (kW)	584
Boiler nominal efficiency (%)	98.2
Distribution thermal losses (%)	15
Water temperature at the boiler outlet (°C)	80
Cooling system (air-to-air heat pumps)	
Temperature setpoint (°C)	26
Nominal EER	2.16
DHW system (electrical heaters)	
Nominal efficiency, including distribution losses (%)	90
DHW specific demand (L/person)	22
DHW desired temperature (°C)	48
Mean temperature of the cold tap water (°C)	12

2.2. The Renovation Scenario of the Examined Building

In this subsection, the renovation strategy that will be implemented regarding the renovation and transformation of the examined building into a more functional building is analytically described and segmented into specific renovation actions. The renovation strategy's targets are a decrease in the building's energy consumption, an increase in the building's renewable energy sources production, and ultimately an improvement in its energy autonomy [34]. In the renovation scenario, the building's DHW production system is not modified, whereas the building is divided into two thermal zones, served by two different energy systems for heating and cooling.

2.2.1. Ground-Source Heat Pump

A reversible ground-source heat pump (GSHP) partially serves the building's heating and cooling demand using a low-global-warming potential refrigerant. The respective heat pump is coupled with a borehole heat exchanger (BHE) system. This solution has no negative visual impact on the building because of the lack of outdoor units of fossil fuel boilers or air source heat pumps, and it does not deteriorate the acoustic pollution [35] or the summer heat island effect in the urban center. The GSHP heat transfer fluid consists of a mixture of water and glycol that serves as an antifreeze agent, ensuring the system's reliability in extreme cold environmental conditions and facilitating efficient heat exchange with the ground through the BHE system.

The GSHP's technology is integrated with a fan coil system that serves both the heating and cooling needs of 40% of the treated zone in the building. For the heating period, the air temperature setpoint is configured at 20 °C. In the heating mode, the heat transfer fluid in the terminal units is characterized by inlet and outlet temperature levels of 50 °C and 40 °C, respectively, while in the BHE system, the heat transfer fluid is characterized by inlet and outlet temperature levels of -3 °C and 0 °C. Conversely, for the cooling period, there are no specific regulations concerning the period's duration. The control system of the building autonomously determines the energy system's operation, and the air temperature setpoint is configured at 26 °C. In the cooling mode, the heat transfer fluid in the terminal units is characterized by inlet and outlet temperature levels of 7 °C and 12 °C, respectively, while in the BHE system, the heat transfer fluid is characterized by inlet and outlet temperature levels of 35 °C and 30 °C. Table 5 includes technical data referring to the GSHP's operational efficiency and temperature levels, retrieved from the technological solution of Eneren [36]. The distribution losses of the energy system's configuration (on the building side) are considered to be equal to 10% for both the heating and cooling operations.

Table 5. Technical data of the GSHP energy system.

Parameter	Value
Heating mode	
Nominal source inlet temperature (°C)	-3
Nominal source outlet temperature (°C)	0
Nominal terminal unit inlet temperature (°C)	50
Nominal terminal unit outlet temperature (°C)	40
Nominal COP	2.83
Nominal heating capacity (kW)	248.9
Compressor isentropic efficiency (%)	55.2
Cooling mode	
Nominal source inlet temperature (°C)	35
Nominal source outlet temperature (°C)	30
Nominal terminal unit inlet temperature (°C)	7
Nominal terminal unit outlet temperature (°C)	12
Nominal EER	3.94
Nominal heating capacity (kW)	295.1
Compressor isentropic efficiency (%)	55.2

2.2.2. Borehole Thermal Energy Storage System

The BHEs' field design consists of $20\text{ m} \times 150\text{ m}$ deep parallel double-U BHEs organized in a rectangular layout with 7 m spacing between the boreholes. According to local geological and hydrogeological data, the initialization values of the ground temperature are assumed to be $14\text{ }^{\circ}\text{C}$, and the vertical temperature gradient is 0.03 K/m . Thermal properties and other specifications concerning the BHEs' configuration and the tubing system [36], as well as the surrounding soil, are demonstrated in Table 6.

Table 6. Borehole thermal energy storage system specifications.

Borehole Parameters	Values
Ground mean temperature ($^{\circ}\text{C}$)	14
Number of parallel boreholes (conventional grouting)	20
Borehole distance (m)	7
Borehole depth (m)	150
Radius of each borehole (m)	0.075
Thermal conductivity of filling material for grouting (W/mK)	1.6
Grouting volume [m^3]	2.65
Soil Characteristics	
Thermal conductivity (W/mK)	2.30
Heat capacity ($\text{MJ/m}^3\text{K}$)	2.16
Geothermal heat flow (W/m^2)	0.06
Tubing System Specifications	
Radius of the tubes (mm)	16
Thickness of the tubes (mm)	3

For the province of Trento, several studies have focused on the geo-exchange potential of vertical closed-loop systems, using Spatial and Geographical Information System tools [37], experimental geothermal monitoring, numerical modeling, and multi-scale/multi-method geological surveys. It is worth mentioning that the most recent Provincial Energy–Environmental Plan has highlighted the strategic role of sector coupling among large-scale hydroelectric production and the electrification of thermal and transport demands (heat pumps, electric mobility). This strategic role of heat pumps in local decarbonization scenarios has been modeled not only on a provincial scale but also on a local scale [38].

2.2.3. Building-Integrated Photovoltaic System

Building-integrated photovoltaic (BIPV) shingles are slim and flexible bituminous-based lightweight photovoltaic (PV) shingles suitable for applications in complicated building roof geometries. Their cells are made of triple-junction thin-film amorphous silicon that absorbs blue, green, and red light through three separate layers, producing energy with direct and diffuse light. Bypass diodes between the cells allow each module to produce energy even when it is partially in the shade. Table 7 lists the data concerning a PV module of 144 W nominal maximum power production obtained from the manufacturer data sheets of Tegosolar [39] referring to standard test conditions. The respective technology is installed on the south roof of the neighboring gym, covering a roof area of 305 m^2 . In total, the PV panels installed are equal to 140 panels of 20.16 kW maximum power production. The PV field is characterized by an azimuth angle of -10° and a tilt angle of 10° .

Table 7. Technical data specifications of the BIPV system.

Parameter	Value
Module length (m)	5.412
Module width (m)	0.373
Number of cells	22
Open-circuit voltage— V_{oc} (V)	46.2
Short-circuit current— I_{sc} (A)	5.3
Maximum power point (W)	144
Temperature coefficient of I_{sc} (%/°C)	0.1
Temperature coefficient of V_{oc} (%/°C)	-0.38

2.2.4. Insulation of the Roof

The building's roof is covered with a layer of insulation, characterized by a thickness of 18 cm and a thermal conductivity value of 0.036 W/mK. This renovation action decreases the roof's thermal transmittance value from 0.5 W/m²K to 0.2 W/m²K. The insulation will be installed on the interior surface of the building, so there will not be any visual change in the building's exterior.

2.2.5. Replacement of the Windows

The building's windows are replaced with double-glazed windows, characterized by a total thermal transmittance value of 1.3 W/m²K and a heat gain coefficient of 0.6. The new windows will be selected to avoid any visual change to the building's exterior; therefore, similar colors and materials to the existing ones will be selected.

2.2.6. Installation of Standard PV Panels

A total roof surface of 300 m² is covered with standard PV panels, characterized by a panel surface of 1.76 m². These panels are installed on the neighboring auditorium's roof, with a south orientation (-10°) and an inclination of 10°. The PV field's maximum power production is equal to 57 kW. Table 8 gives the technical data of the Aleo PV panels [39] with 330 W nominal maximum power production used in the present analysis.

Table 8. Technical characteristics of the PV panel system.

Parameters	Values
Panel surface (m ²)	1.76
Open-circuit voltage— V_{oc} (V)	40.8
Short-circuit current— I_{sc} (A)	10.7
Maximum power point (W)	330
Temperature coefficient of I_{sc} (%/°C)	+0.05
Temperature coefficient of V_{oc} (%/°C)	-0.29

2.2.7. Installation of an LED Lighting System

The entire building's lighting system is replaced with an LED lighting system, decreasing the specific lighting load from 9 W/m² to 5 W/m², and therefore reducing the building's electricity consumption through its lighting.

2.3. Basic Mathematical Modeling

The thermal transmittance (U-value) of the structural components (wall, roof, ground slab, etc.) is given as follows [40]:

$$U = \frac{1}{h_{out} + \sum \left(\frac{t_i}{k_i} \right) + h_{in}} \quad (1)$$

where (i) represents the different layers of each structural component. The heat convection coefficients were selected according to ISO 6946:2017 [41], and they are $h_{in} = 7.7 \text{ W/m}^2\text{K}$ and $h_{out} = 25 \text{ W/m}^2\text{K}$.

The thermal transmittance (U-value) of windows is given as follows [40]:

$$U = \frac{U_{window} \cdot A_{window} + U_{glass} \cdot A_{glass}}{A_{window} + A_{glass}} \quad (2)$$

In the previous equation, the frame and window parameters (i.e., area and thermal transmittance) are used.

The fuel energy demand of the boiler (Q_b) is calculated by using the heating load (Q_{heat}), the boiler efficiency (η_{boiler}), and the distribution thermal loss efficiency ($\eta_{dis,boiler}$):

$$Q_b = \frac{Q_{heat}}{\eta_{boiler} \cdot \eta_{dis,boiler}} \quad (3)$$

The condensing boiler's nominal efficiency is selected to be ($\eta_{boiler} = 98\%$), and the distribution thermal loss efficiency is selected to be ($\eta_{dis,boiler} = 85\%$). More details about the boiler modeling with INTEMA.building can be found in Ref. [33].

Regarding the split units (air-to-air heat pumps) for cooling in the baseline scenario, the nominal EER was selected at 2.16 because they are old units, and the respective electricity consumption is calculated as follows:

$$P_{el,cool,split} = \frac{Q_{cool}}{EER_{split}} \quad (4)$$

For the renovation scenario with the geothermal heat pump, the nominal heating COP is selected to be 2.83 and the nominal cooling EER is selected to be 3.94. Also, the distribution losses from the heat pumps to the fan coils are estimated by using the distribution thermal loss efficiency ($\eta_{dis,fancoil}$), which is assumed to be 90%. This distribution efficiency is greater than the case of the boiler with radiators because the fan coils operate at lower temperatures. In these cases, the electricity consumption for heating and cooling is calculated as below:

$$P_{el,heat,geoth} = \frac{Q_{heat}}{\eta_{dis,fancoil} \cdot EER_{geoth}} \quad (5)$$

$$P_{el,cool,geoth} = \frac{Q_{cool}}{\eta_{dis,fancoil} \cdot EER_{geoth}} \quad (6)$$

A detailed modeling of the ground-source heat pump with the INTEMA.building tool can be found in Ref. [42].

The electricity production of the PV panels ($P_{el,PV}$) is calculated by using the electrical efficiency of the PV panels (η_{el}), the PV panels' area (A_{PV}), and the incident solar irradiation on the PV panels (G_T):

$$P_{el,PV} = \eta_{el} \cdot A_{PV} \cdot G_T \quad (7)$$

The modeling of the PV panels is based on the equivalent circuit of a two-diode model cell, and more details of this can be found in Refs. [43,44]. Moreover, this model has been used in our previous work with INTEMA.building [33].

2.4. Simulation Strategy

The simulation software used for the current numerical study is INTEMA.building, a customized dynamic simulation tool developed using the Modelica language [28] and the Dymola modeling and simulation environment, including a graphical user interface and a solver [29]. The distinctive feature of this tool is rooted in its capacity to simulate complicated and detailed energy system configurations with accuracy through the utilization and combination of simpler and modular subcomponents. The simulations are

realized with adjustable time steps to account for strongly fluctuating variables in the analysis, such as those triggered by the implementation of control systems. This method guarantees a highly realistic framework for the acquired results. For the present analysis, the basic timestep is set to be 1 h, wherein the solver user is the Dassl solver [45] with 10^{-4} tolerance. The INTEMA.building tool has been used in various studies investigating the thermal performance of buildings and the operation of their energy systems [33,42,46] by the authors of this paper. Additionally, the respective tool has also been compared with the TRNSYS 18 simulation software [33] and validated according to the European Standard EN15265 [47].

The baseline scenario includes one energy system (ESC 1), which is depicted in Figure 5. On the other hand, the renovation scenarios use two energy systems (ESC 1, ESC 2): the old system in Figure 5 and the new one in Figure 6. Practically, the renovation scenario includes a partial renovation of the energy system because there is not enough capacity in the ground-source heat pump to serve the entire building.

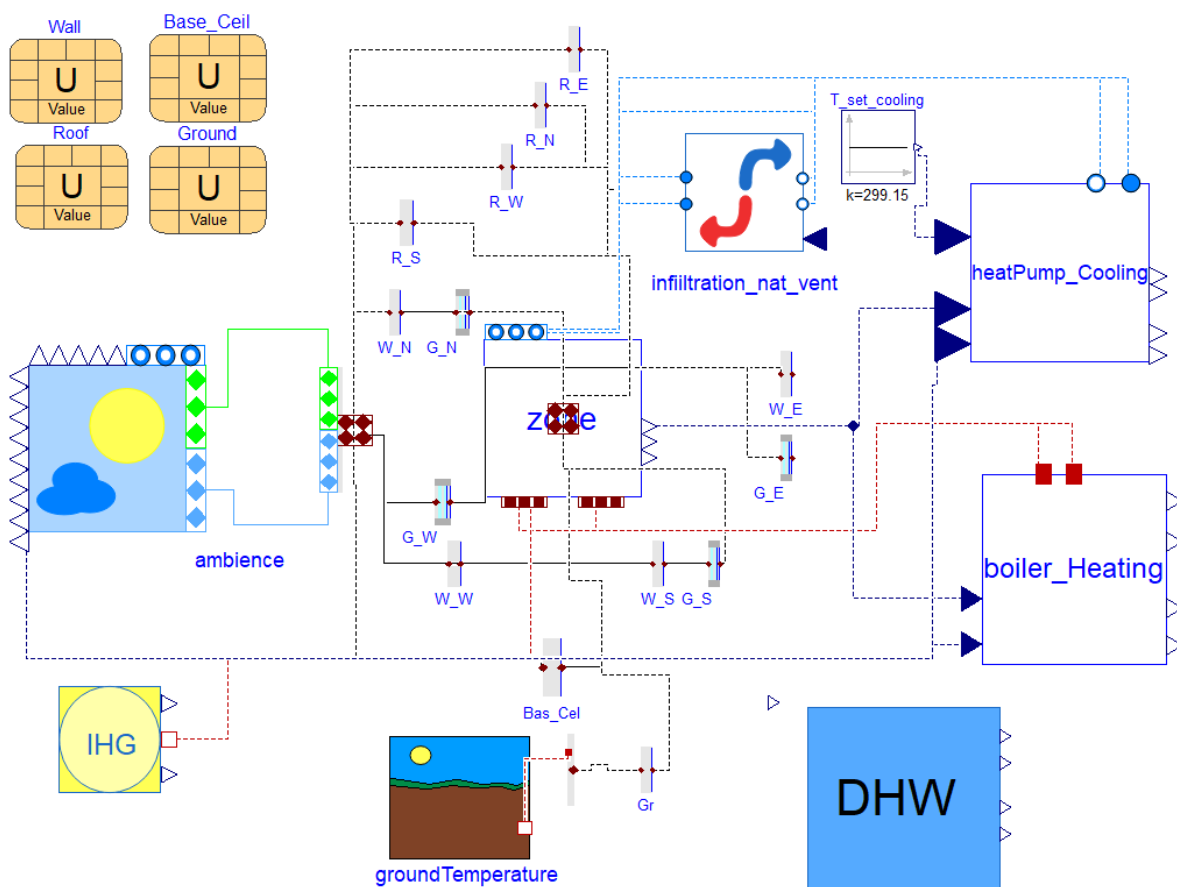


Figure 5. Configuration of ESC 1 coupled with the examined building in the Modelica environment.

The layout of the building with a space heating system, a cooling system, and the DHW system for the baseline scenario is depicted in Figure 5. More specifically, the essential components that comprise the total system are depicted, as well as their basic connections. In the baseline scenario, the entire treated floor area of the building is served by a single heating system composed of condensing gas boilers coupled with the radiators distributed throughout the entire building, a single cooling system composed of air-to-air heat pump split units, and DHW production systems composed of local electrical heaters. The respective heating, cooling, and DHW system combination is referred to as energy system configuration 1 (ESC 1).

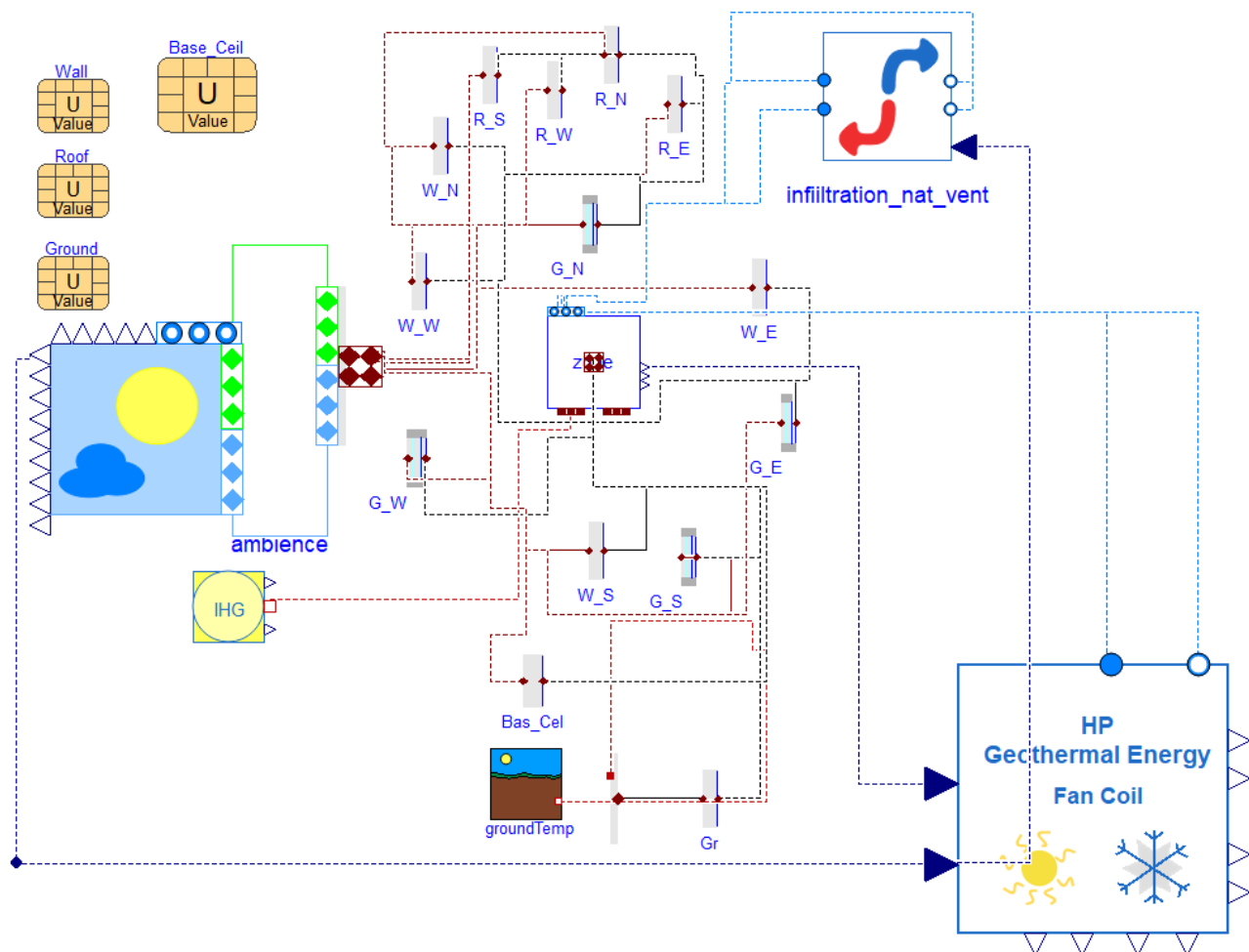


Figure 6. Configuration of ESC 2 coupled with the examined building in the Modelica environment.

Practically, Figure 5 includes the building envelope and the energy systems. The building envelope is modeled by using the central component of the thermal zone where the energy balances are conducted in every time step. The external structural components (walls, roof, windows, etc.) are coupled with the thermal zone in order to simulate the energy exchange between the thermal zone and the ambient air. There is also a specific component for infiltration/ventilation, a specific component for the internal loads, and a component for the heat exchange with the ground. Regarding the energy systems, there are components for the DHW, a boiler for covering the heating loads, and a conventional heat pump for covering the cooling loads.

Conversely, in the renovation scenario, the building is served by a combination of heating and cooling systems, whereas no alterations are realized regarding the DHW production system. In the respective scenario, 60% of the building-covered floor area is served by the heating and cooling system of the baseline scenario, namely the gas boiler system coupled with radiators for heating and the heat pump split units for cooling. The remaining 40% of the building's treated floor area is served by the integration of GSHPs and BHEs coupled with the fan coil system, serving both the building's heating and cooling needs, referred to as energy system configuration 2 (ESC 2). Figure 6 depicts the configuration of 40% of the building served by ESC2 developed in the Modelica environment. Specifically, Figure 6 shows the new thermal zone, which is served by one energy system, which is the innovative GSHP system. The rest of the components regarding the building envelope are similar to the baseline case, but they have been properly adjusted to the examined renovated thermal zone.

Additionally, Figure 7a illustrates the integration of the developed components of GSHP system and the fan coil system, as well as their basic connections, while Figure 7b represents the component of the water-to-water reversible heat pump connected with the component of the geothermal field of the BHEs. Specifically, Figure 7a illustrates the connection of the heat pump with the fan coil and the total configuration including circulating pumps, a control unit, thermometers, and piping components. Figure 7b shows the connection of the heat pump with the ground boreholes, and it includes a thermometer and a flowmeter in the given depiction.

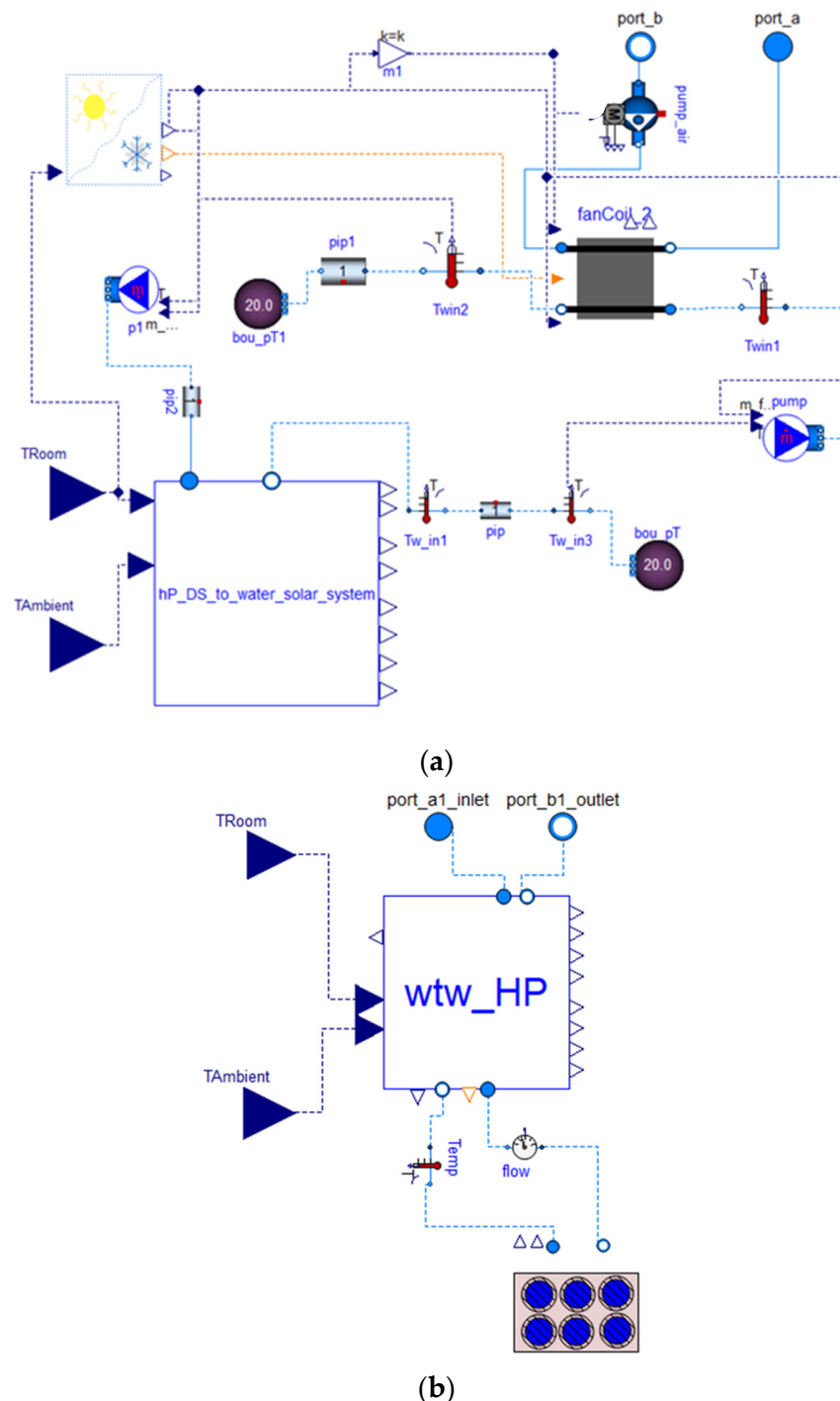


Figure 7. Detailed configuration of ESC 2: (a) GSHP coupled with the fan coil system, and (b) water-to-water reversible heat pump coupled with the BHE system.

3. Results and Discussion

This section includes the simulation results for the baseline scenario and the investigation of the renovation scenarios. Also, a comparison of both scenarios in terms of energy is given in the last part of this section.

3.1. Energy Analysis of the Baseline Scenario

Firstly, the results of the dynamic simulations regarding the baseline scenario are presented. Specifically, Figure 8a depicts the heating energy load and cumulative energy demand of the examined building, while Figure 8b shows the boiler's power and cumulative energy demand during the heating season. According to the simulation results, the yearly demand for fuel consumed by the natural gas boiler is calculated to be 914,352 kWh, covering a heating load of 762,866 kWh. Moreover, Figure 9a depicts the cooling energy load and cumulative energy demand, while Figure 9b illustrates the electrical load and cumulative electrical energy demand of the building. The calculated yearly cooling demand is 55,762 kWh, while the respective consumed electricity is 25,816 kWh. It is important to highlight that the cooling needs are significantly lower than the heating needs because the examined location presents relatively low temperature levels, especially during the winter. Additionally, Figure 10 depicts the indoor and ambient air temperatures during the year. The temperature setpoint of 20 °C and the desired thermal comfort conditions are not satisfied during short periods in May and September due to the definition of the six-month heating season (14 October–16 April).

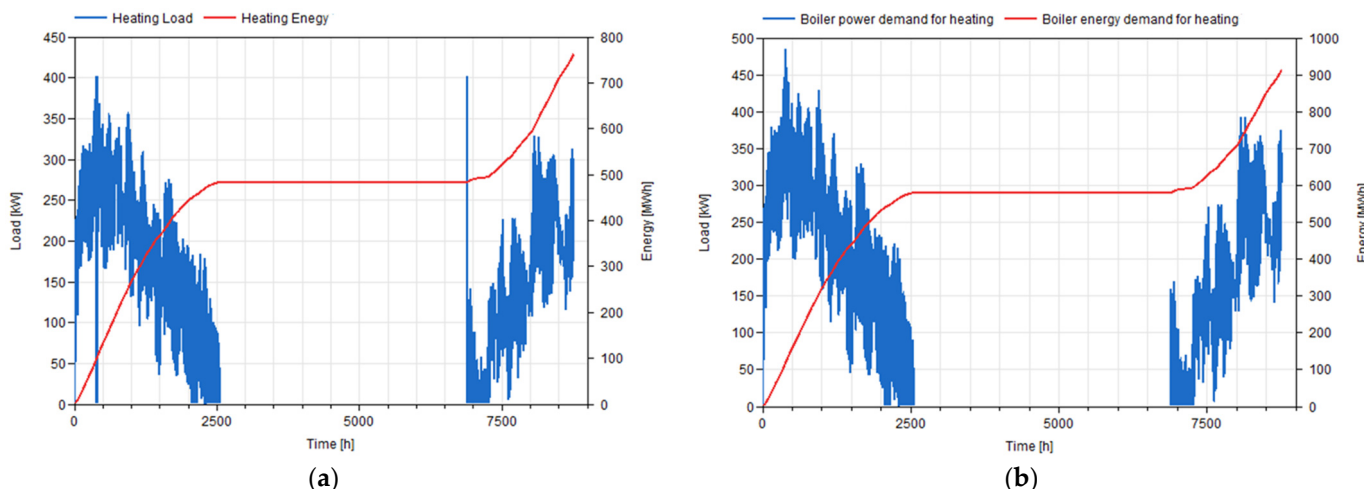


Figure 8. (a) Heating energy load and cumulative heating energy demand, (b) Boiler power and cumulative boiler energy demand for heating.

As far as the DHW production system is concerned, Figure 11a depicts the DHW energy load and cumulative energy demand, whereas Figure 11b illustrates the electrical power and cumulative electricity consumption of the local electrical DHW heaters. The calculated yearly energy demand for DHW is 67,241 kWh, while the respective electricity demand for its preparation is 74,653 kWh. Moreover, the yearly demand for DHW is around 1606 m³ of water. These results refer to the baseline as well as the renovation scenario, since no alterations have been realized regarding the building's DHW production system. Finally, Figure 12 depicts the electricity power and cumulative energy demand for covering the yearly needs of the appliances and the lighting. This quantity is computed to be 267,502 kWh.

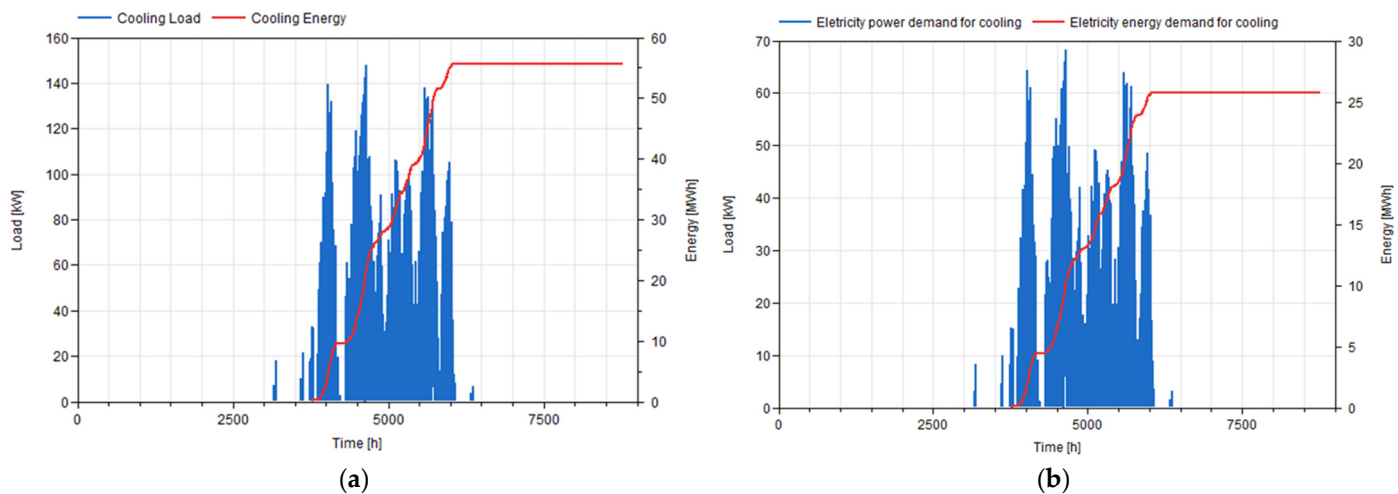


Figure 9. (a) Cooling energy load and cumulative heating energy demand. (b) Heat pump's electrical power and cumulative electrical energy demand for cooling.

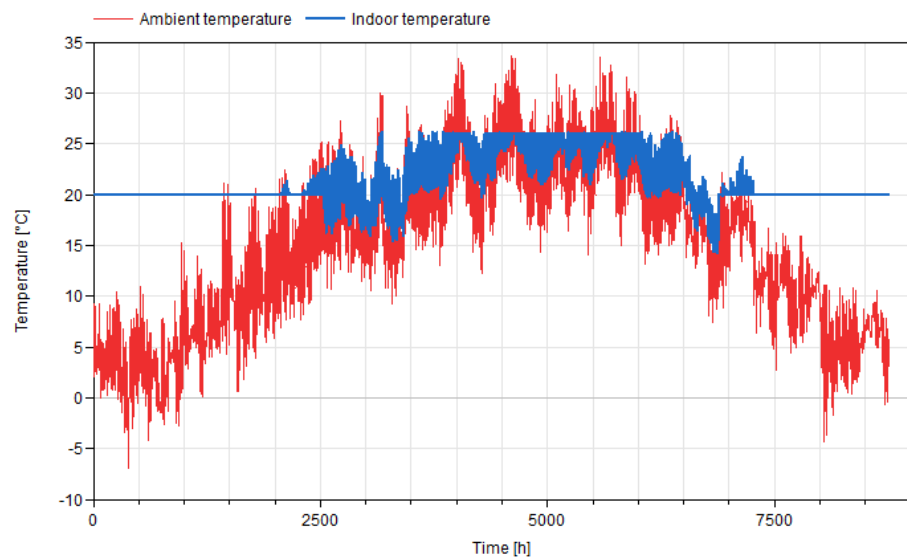


Figure 10. Indoor air temperature and ambient air temperature levels.

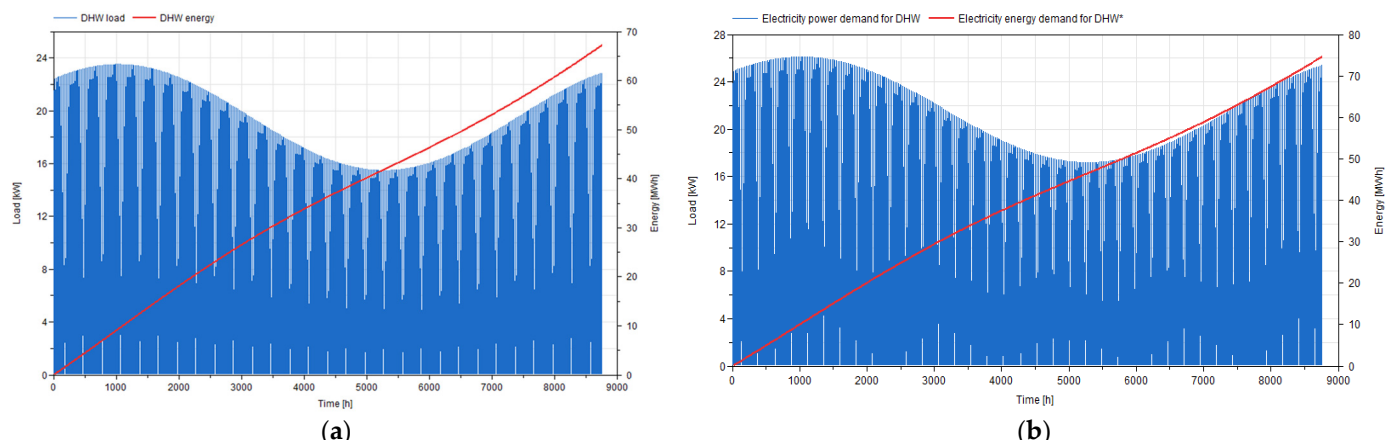


Figure 11. (a) DHW energy load and cumulative DHW energy demand. (b) Electrical power and cumulative electrical energy demand for DHW production.

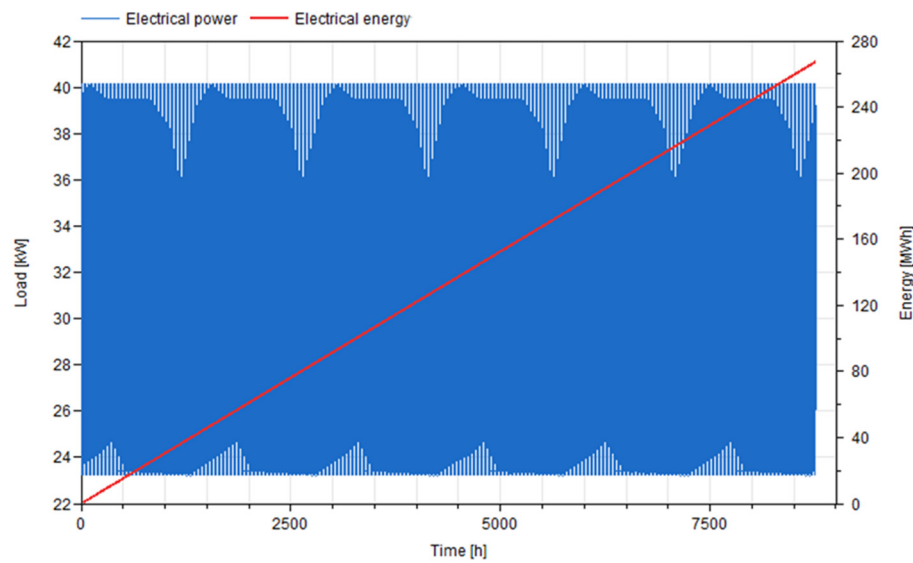
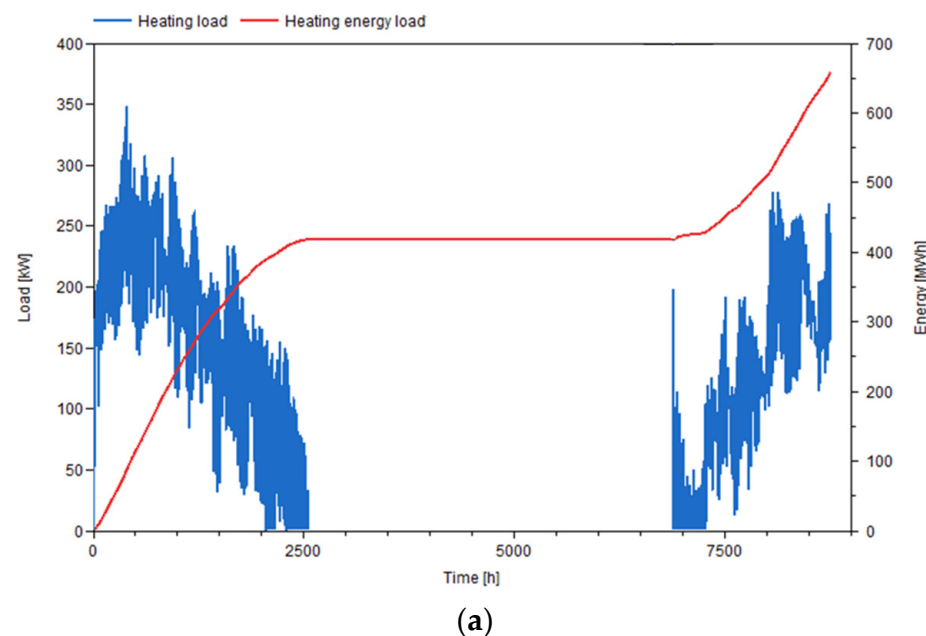


Figure 12. Electricity power and cumulative energy demand for covering the needs of the appliances and the lighting in the baseline scenario.

3.2. Energy Analysis of the Renovation Scenario

In the present subsection, the results of the dynamic simulations regarding the renovation scenario are discussed. Firstly, regarding the heating season, Figure 13a depicts the entire building's heating load and cumulative heating energy load, a value that is calculated at 658,079 kWh. Specifically, for the building zone served by the heating systems of ESC 1, corresponding to 60% of the building's total treated floor area, the cumulative heating energy demand is calculated to be 396,841 kWh, whereas for the building zone served by the systems of ESC 2, this respective value is equal to 261,238 kWh. Additionally, Figure 13b illustrates the natural gas boiler's power and yearly energy demand, a value which is calculated to be 475,325 kWh, while Figure 13c depicts the electrical power and yearly electricity demand of the GSHPs for heating, which is found to be 102,603 kWh.



(a)

Figure 13. Cont.

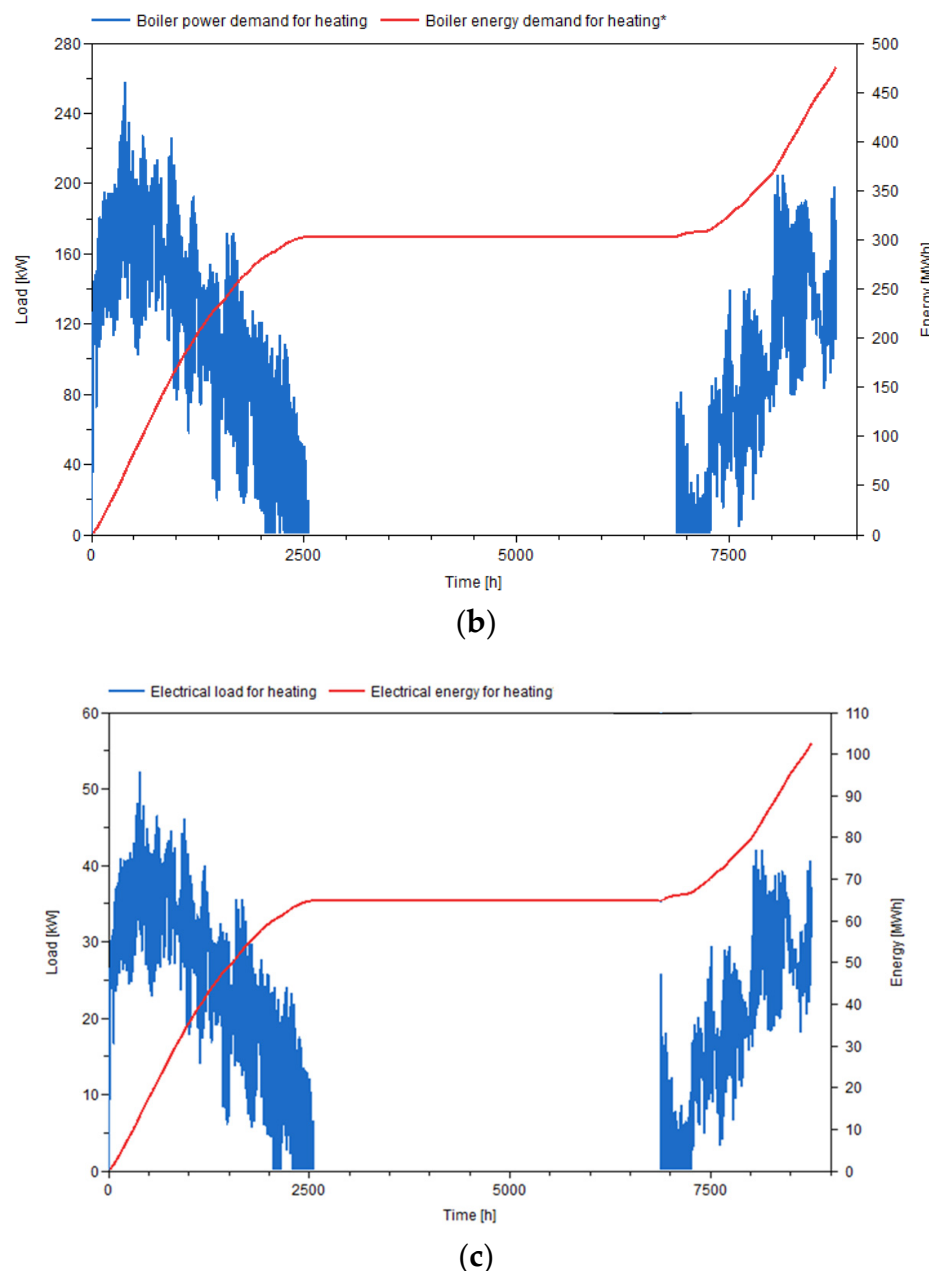


Figure 13. (a) Heating load and cumulative heating energy load of the entire building. (b) Boiler power and cumulative boiler energy demand for heating in ESC 1. (c) Electrical power and electrical cumulative energy demand for heating in ESC 2.

Moreover, as far as the building's cooling demand is concerned, Figure 14a depicts the entire building's cooling load and cumulative cooling energy load, which is calculated to be 52,126 kWh. Regarding the ESC 1 cooling scenario, the cumulative cooling energy load is calculated to be 33,859 kWh, while according to Figure 14b, the corresponding electricity consumption of the air-to-air heat pump split units is calculated at 15,676 kWh. On the other hand, for the ESC 2 cooling scenario, the cumulative cooling energy load is calculated at 18,267 kWh, while according to Figure 14b, the corresponding electricity consumption of the air-to-air heat pump split units is calculated at 5166 kWh. Additionally, Figure 15 depicts the ambient air and building zones' indoor air temperature levels.

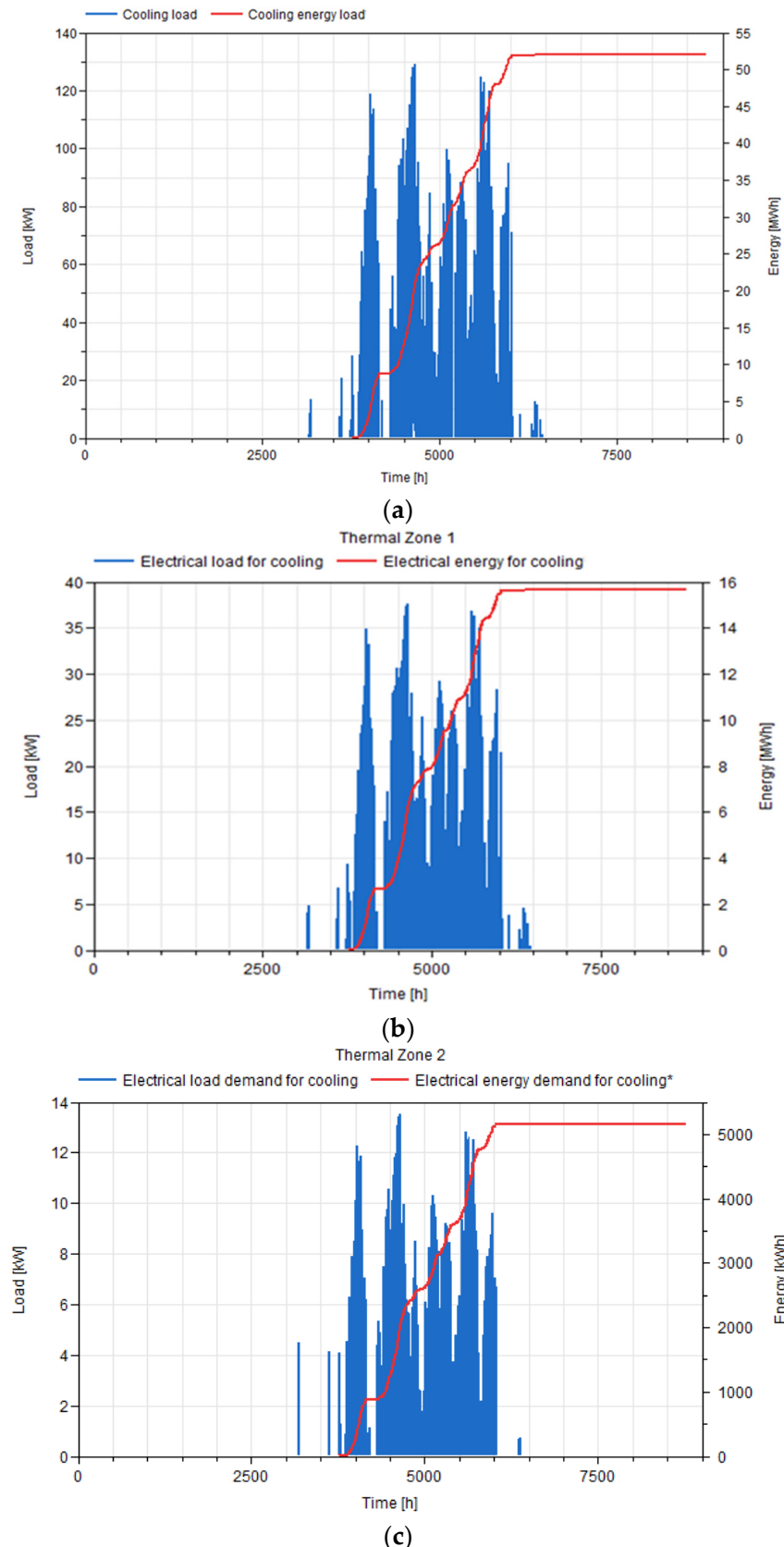


Figure 14. (a) Cooling load and cumulative cooling energy load of the entire building. (b) Electrical power and cumulative electrical energy demand for cooling in ESC 1. (c) Electrical power and cumulative electrical energy demand for cooling in ESC 2.

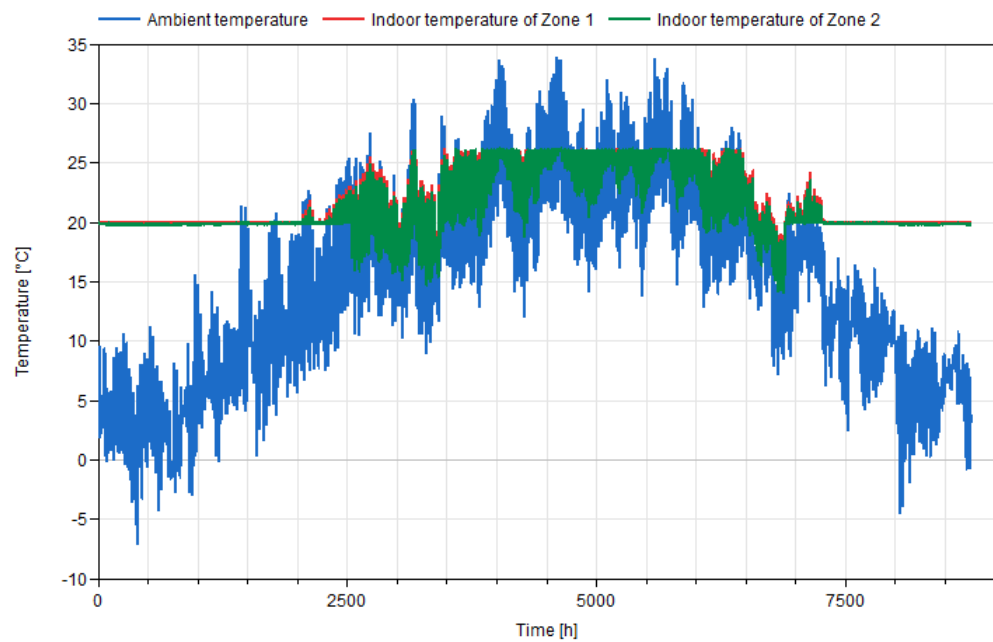


Figure 15. Ambient temperature and indoor temperature of building zones served by ESC 1 and ESC 2.

The installation of the LED lighting system affects the building's electricity demand for appliances and lighting, according to Figure 16. Specifically, the cumulative electricity demand for these purposes is calculated at 236,915 kWh. As far as the electricity production is concerned, according to the calculations and Figure 17a, the total electricity produced by the BIPV field installed on the neighboring gym is equal to 24,293 kWh. Additionally, Figure 17b illustrates the electricity production from the standard PV field installed in the neighboring auditorium, calculated at 74,832 kWh.

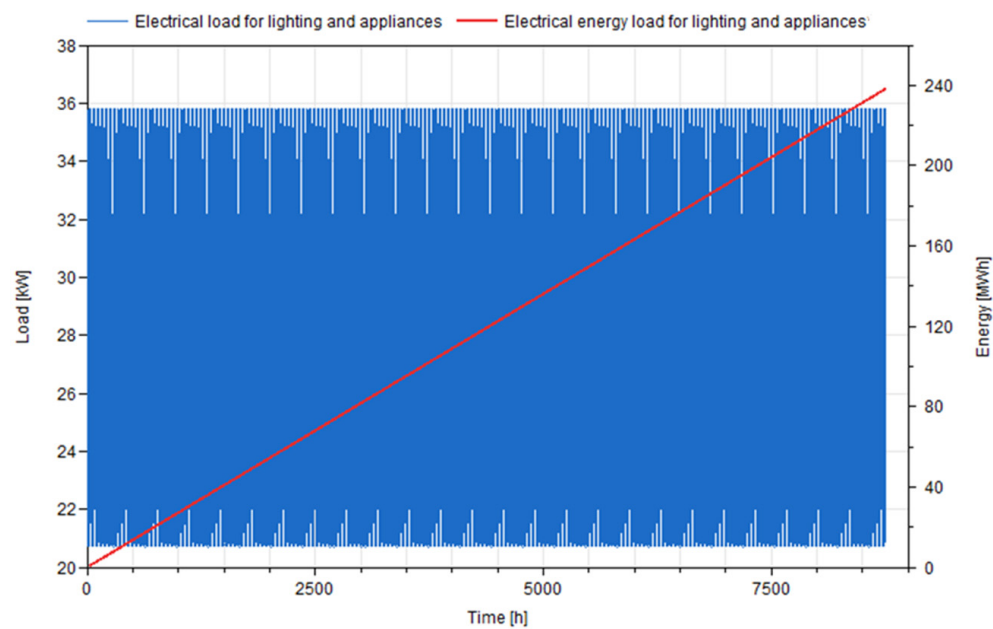


Figure 16. Electricity power and cumulative energy demand for covering the needs of the appliances and the lighting in the renovation scenario.

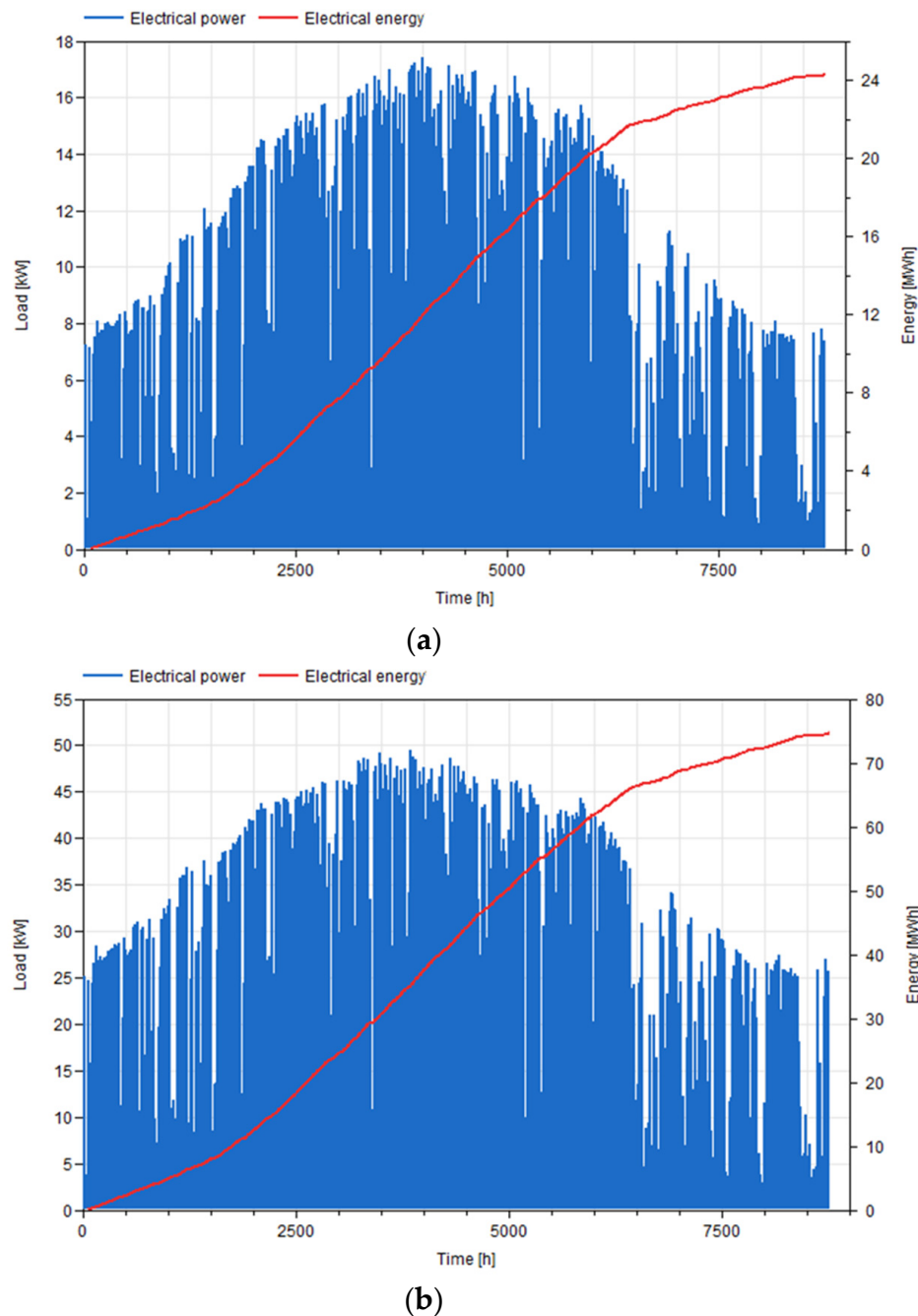


Figure 17. Electrical power and electrical energy produced by (a) the BIPV system and (b) the standard PV field.

3.3. Discussion

This section compares and briefly discusses the simulation results regarding the baseline and renovation scenarios. The purpose of the renovation strategy for the examined building is to decrease its thermal loads and improve the thermal comfort conditions of its occupants. To achieve that, various standards, as well as technologically advanced solutions, are implemented. The energy simulation analysis conducted in this report allows for the comparison between the two states of the building and the prediction of the energy savings induced by the renovation actions. In Table 9, the basic yearly energy demands of each examined scenario, as well as the energy efficiency indexes of the studied heating and cooling systems, are given.

Table 9. Comparison of basic energy demands between the baseline and renovation scenarios on a yearly basis.

Parameters	Baseline [kWh]	Renovation [kWh]	Difference [%]
Heating energy demand	762,866	658,079	-13.74%
Cooling energy demand	55,762	52,126	-6.52%
Energy demand for DHW	67,241	67,241	0%
Electrical energy for appliances and lighting	267,502	236,915	-11.43%
Natural gas boiler energy demand for heating	914,352	475,325	-48.02%
Electricity consumption for heating	0	102,603	-
Electricity consumption for cooling	25,816	20,842	-19.27%
Electricity consumption for DHW	74,653	74,653	0%
Electricity production of BIPVs	0	24,293	-
Electricity production of standard PV panels	0	74,832	-
Total electricity production	0	99,125	-
Total gross electricity demand	367,971	435,013	18.22%
Total net electricity demand	367,971	335,888	-8.72%
Total primary energy demand	1,650,294	1,147,101	-30.49%
Total final energy demand	1,282,323	811,213	-36.74%

In the baseline scenario, the heating energy demand is calculated at 762,866 kWh, whereas in the renovated state, the heating demand of the building is calculated at 658,079 kWh. This decrease in the heating energy load of the building is combined with the improvement of the living conditions and is equal to 13.74%. In addition, the natural gas boilers' demand is greatly decreased. More specifically, in the baseline scenario, the natural gas boilers' energy demand for heating is calculated to be 914,352 kWh, while for the renovation scenario, this value is equal to 475,325 kWh, which corresponds to a 48.02% reduction. This is explained by the fact that, in parallel with the renovation actions, in the baseline scenario, the heating system in ESC 1 serves the entire building, whereas, in the renovation scenario, the respective heating system serves only 60% of the studied building. Simultaneously, the building's cooling energy loads are also reduced. Precisely, the cumulative cooling energy demand for the baseline scenario is calculated at 55,762 kWh, whereas for the renovation scenario, this value is reduced to 52,126 kWh, indicating a decrease of 6.52%. Regarding the total electricity consumption for cooling, this value is calculated at 25,816 kWh for the baseline scenario. For the renovation scenario, though, applying a combination of the cooling systems in ESC 1 and ESC 2, the total electricity consumption required for cooling is reduced to 20,842 kWh.

Furthermore, in the renovation scenario, the building is equipped with two PV systems, which assist in the reduction of the building's net electricity consumption—specifically, the total electricity produced by the BIPV system and standard PV field aggregates to 99,125 kWh. The electricity production that stems from the installation of the RES systems and the electricity savings achieved with the LED lighting system outweigh the electricity demand of the building's energy systems for heating and cooling in the renovation scenario, resulting in a decrease in the net electricity consumption of the building. Specifically, the building's net electricity consumption is computed to be 335,888 kWh for the renovation scenario, a value indicating an 8.72% decrease compared to the baseline scenario. Finally, as far as the primary energy demand is concerned, for Italy, the primary energy factors are selected at 2.0 for electricity [48] and at 1.0 for natural gas. The renovation strategy applied in the examined building is predicted to result in a 30.49% reduction in the building's primary energy demand.

Moreover, the energy-related renovation of cultural heritage buildings leads to side-line gains as well. Specifically, the increase in the thermal comfort conditions inside the building and reduction in the thermal bridges can decrease the internal humidification in the walls/roof. Also, the high peak temperatures in the summer can lead to thermal stresses and consequently damage the external appearance of the building.

Considering the architectural, legislative, and physical limitations of the present deep renovation, this research proposes a significant reduction of 30.49% in the building's primary energy demand compared to the problematic EU energy efficiency renovation yearly rate of 0.2% [49]. Moreover, the examined renovation strategy respects the historical status of the building and the respective surrounding area, reducing the total primary energy to 50 kWh/m³ per year: a fact that places the examined building among the 40% of public buildings in Trento with low energy consumption [26].

The significant reductions in the building's total primary energy demand (−30.49%) and total final energy demand (−36.74%) align with Italy's national energy objectives, aiming to reduce the total primary energy consumption by 24–43% in the period of 2020–2030 compared to the PRIMES 2007 scenario [50,51]. Moreover, according to the results of the present study, the electricity produced by PV technologies integrated into the examined building covers 22.8% of the building's electricity needs. Taking into consideration the aerothermal and geothermal contributions to the heating and cooling of the building (40% of the building's treated floor area is served by the integration of GSHPs and BHEs), the overall share of renewable energy sources in the building's energy consumption satisfies the national objectives (for the 2020–2030 period, these objectives expect a 17–30% share of the gross final consumption of energy to come from renewable energy sources).

4. Conclusions

The renovation of buildings with cultural heritage significance is a critical aspect in the design of decarbonized sustainable cities. These renovations have both energy-related and social benefits and are characterized as urgent due to the intense climate crisis and the aforementioned unsustainable incumbent building stock.

The present analysis focuses explicitly on an energy-related investigation into the renovation process of a cultural heritage building in the Municipality of Trento in Italy. The selection of this location and this building status constitutes a significant research insight, as Italy, specifically Trento, showcases a critical issue regarding its stock of energy-inefficient historical buildings [52]. Moreover, the historical heritage profile of the examined building challenges the integration of a deep renovation strategy due to architectural and legislative limitations and the need to preserve the building's historical timeline.

This investigation was conducted with the novel dynamic simulation tool INTEMA.building, which is based on the Modelica programming language. The renovation strategy involves a combination of passive and active actions. Below, the most important conclusions of this energy analysis are briefly presented:

- The results indicate that even in a quite challenging building typology (an old protected building, with different uses and common areas), there are solutions that can have a very positive impact in terms of energy performance.
- The building envelope renovation actions discussed in this study reduce the heating and cooling loads of the building by about 13.74% and 6.52%, respectively.
- In the renovation scenario, a reduction of approximately 48% in the natural gas consumption is achieved through the use of a ground-source heat pump.
- The total electricity produced by the PV and the BIPV systems is calculated at 99.1 MWh, covering 22.8% of the building's electricity needs in the renovation scenario.
- The implementation of the renovation strategy is calculated to result in a 30.49% reduction in the primary energy demand, a 36.74% reduction in the final energy demand, and an 8.72% decrease in the net electricity demand.

In the future, an evaluation of the social benefits of the present renovation strategy can be conducted. Additionally, the economic and environmental benefits can be calculated to obtain an overall view of the renovation process of the present case study.

Author Contributions: N.Z.: methodology, software, investigation, writing—original draft preparation; A.K.: methodology, software, investigation, writing—original draft preparation; E.B.: conceptualization, methodology, software, investigation, writing—original draft preparation; P.I.: con-

ceptualization, methodology, writing—original draft preparation; D.G.: software, investigation, writing—original draft preparation; K.A.: conceptualization, supervision, writing—original draft preparation; N.N.: supervision, writing—original draft preparation; S.R.: resources, supervision, writing—original draft preparation; D.V.: resources, supervision, writing—original draft preparation. All authors have read and agreed to the published version of the manuscript.

Funding: This work has been carried out as part of the European Union's Horizon Europe program framework under grant agreement No. 101069610 (InCUBE—An INCIUsive toolBox for accElerating and smartening deep renovation).

Institutional Review Board Statement: Not applicable.

Informed Consent Statement: Not applicable.

Data Availability Statement: Data are available upon request.

Conflicts of Interest: The authors declare that there are no conflicts of interest.

Nomenclature

A	Area, m ²
COP	Heating mode coefficient of performance
E	Energy, kWh
EER	Cooling mode coefficient of performance/Energy Efficiency Ratio
g	Solar heat gain factor for the windows
G _T	Incident solar irradiation, W/m ²
h _{in}	Inside convection coefficient, W/m ² K
h _{out}	Outside convection coefficient, W/m ² K
I	Current, A
k	Thermal conductivity, W/mK
P _{el}	Electrical energy, kWh
PV	Photovoltaic
Q	Thermal load, W
t	Layer thickness, m
U	Thermal transmittance, W/m ² K
V	Voltage, V

Subscripts and Superscripts

b	Boiler
cool	Cooling
dis	Distribution thermal losses
el	Electricity
frame	Window's opening frame
geoth	Geothermal
glass	Window's glass
heat	Heating
max	Maximum
oc	Open-circuit
sc	Short-circuit
split	Heat pump split units

Greek symbols

γ	Azimuth angle, °
η	Efficiency

Abbreviations

ACH	Air changes per hour
BHE	Borehole heat exchanger
BIPV	Building-integrated photovoltaic
DHW	Domestic hot water
ESC	Energy system configuration for heating, cooling, and DHW purposes
GSHP	Ground-source heat pump
HVAC	Heating, cooling, and air-conditioning

References

1. Lidelöw, S.; Örn, T.; Luciani, A.; Rizzo, A. Energy-Efficiency Measures for Heritage Buildings: A Literature Review. *Sustain. Cities Soc.* **2019**, *45*, 231–242. [CrossRef]
2. Zhang, Y.; Teoh, B.K.; Wu, M.; Chen, J.; Zhang, L. Data-Driven Estimation of Building Energy Consumption and GHG Emissions Using Explainable Artificial Intelligence. *Energy* **2023**, *262*, 125468. [CrossRef]
3. European Parliament and the Council of the European Union. Directive (EU) 2023/1791 of the European Parliament and of the Council of 13 September 2023 on energy efficiency and amending Regulation (EU) 2023/955. Available online: <https://eur-lex.europa.eu/eli/dir/2023/1791/oj> (accessed on 11 January 2024).
4. Zhu, X.; Zhang, X.; Gong, P.; Li, Y. A Review of Distributed Energy System Optimization for Building Decarbonization. *J. Build. Eng.* **2023**, *73*, 106735. [CrossRef]
5. Kataray, T.; Nitesh, B.; Yarram, B.; Sinha, S.; Cuce, E.; Shaik, S.; Vigneshwaran, P.; Roy, A. Integration of Smart Grid with Renewable Energy Sources: Opportunities and Challenges—A Comprehensive Review. *Sustain. Energy Technol. Assess.* **2023**, *58*, 103363. [CrossRef]
6. Semprini, G.; Gulli, R.; Ferrante, A. Deep Regeneration vs Shallow Renovation to Achieve Nearly Zero Energy in Existing Buildings. *Energy Build.* **2017**, *156*, 327–342. [CrossRef]
7. Assimakopoulos, M.-N.; De Masi, R.F.; Fotopoulou, A.; Papadaki, D.; Ruggiero, S.; Semprini, G.; Vanoli, G.P. Holistic Approach for Energy Retrofit with Volumetric Add-Ons toward nZEB Target: Case Study of a Dormitory in Athens. *Energy Build.* **2020**, *207*, 109630. [CrossRef]
8. Moran, F.; Blight, T.; Natarajan, S.; Shea, A. The Use of Passive House Planning Package to Reduce Energy Use and CO₂ Emissions in Historic Dwellings. *Energy Build.* **2014**, *75*, 216–227. [CrossRef]
9. Cho, H.M.; Yun, B.Y.; Yang, S.; Wi, S.; Chang, S.J.; Kim, S. Optimal Energy Retrofit Plan for Conservation and Sustainable Use of Historic Campus Building: Case of Cultural Property Building. *Appl. Energy* **2020**, *275*, 115313. [CrossRef]
10. Ma, Z.; Cooper, P.; Daly, D.; Ledo, L. Existing Building Retrofits: Methodology and State-of-the-Art. *Energy Build.* **2012**, *55*, 889–902. [CrossRef]
11. Arumägi, E.; Kalamees, T. Analysis of Energy Economic Renovation for Historic Wooden Apartment Buildings in Cold Climates. *Appl. Energy* **2014**, *115*, 540–548. [CrossRef]
12. Ardente, F.; Beccali, M.; Cellura, M.; Mistretta, M. Energy and Environmental Benefits in Public Buildings as a Result of Retrofit Actions. *Renew. Sustain. Energy Rev.* **2011**, *15*, 460–470. [CrossRef]
13. Fonseca, D.J.; Bisen, K.B.; Clark Midkiff, K.; Moynihan, G.P. An Expert System for Lighting Energy Management in Public School Facilities. *Expert Syst.* **2006**, *23*, 194–211. [CrossRef]
14. Cohen, S.; Goldman, C.; Harris, J. Energy Savings and Economics of Retrofitting Single-Family Buildings. *Energy Build.* **1991**, *17*, 297–311. [CrossRef]
15. Boait, P.J.; Fan, D.; Stafford, A. Performance and Control of Domestic Ground-Source Heat Pumps in Retrofit Installations. *Energy Build.* **2011**, *43*, 1968–1976. [CrossRef]
16. Hens, H. Energy Efficient Retrofit of an End of the Row House: Confronting Predictions with Long-Term Measurements. *Energy Build.* **2010**, *42*, 1939–1947. [CrossRef]
17. Gravagnuolo, A.; Angrisano, M.; Bosone, M.; Buglione, F.; De Toro, P.; Fusco Girard, L. Participatory Evaluation of Cultural Heritage Adaptive Reuse Interventions in the Circular Economy Perspective: A Case Study of Historic Buildings in Salerno (Italy). *J. Urban Manag.* **2024**, *13*, 107–139. [CrossRef]
18. De Toro, P.; Nocca, F.; Renna, A.; Sepe, L. Real Estate Market Dynamics in the City of Naples: An Integration of a Multi-Criteria Decision Analysis and Geographical Information System. *Sustainability* **2020**, *12*, 1211. [CrossRef]
19. Akkurt, G.G.; Aste, N.; Borderon, J.; Buda, A.; Calzolari, M.; Chung, D.; Costanzo, V.; Del Pero, C.; Evola, G.; Huerto-Cardenas, H.E.; et al. Dynamic Thermal and Hygrometric Simulation of Historical Buildings: Critical Factors and Possible Solutions. *Renew. Sustain. Energy Rev.* **2020**, *118*, 109509. [CrossRef]
20. Ascione, F.; De Rossi, F.; Vanoli, G.P. Energy Retrofit of Historical Buildings: Theoretical and Experimental Investigations for the Modelling of Reliable Performance Scenarios. *Energy Build.* **2011**, *43*, 1925–1936. [CrossRef]
21. Harrestrup, M.; Svendsen, S. Full-Scale Test of an Old Heritage Multi-Storey Building Undergoing Energy Retrofitting with Focus on Internal Insulation and Moisture. *Build. Environ.* **2015**, *85*, 123–133. [CrossRef]
22. Şahin, C.D.; Arsan, Z.D.; Tunçoku, S.S.; Broström, T.; Akkurt, G.G. A Transdisciplinary Approach on the Energy Efficient Retrofitting of a Historic Building in the Aegean Region of Turkey. *Energy Build.* **2015**, *96*, 128–139. [CrossRef]
23. Zagorskas, J.; Palulis, G.M.; Burinskienė, M.; Venckauskaitė, J. Energetic Refurbishment of Historic Brick Buildings: Problems and Opportunities. *Sci. J. Riga Tech. Univ. Environ. Clim. Technol.* **2013**, *12*, 20–27. [CrossRef]
24. Serrano, T.; Kampmann, T.; Ryberg, M.W. Comparative Life-Cycle Assessment of Restoration and Renovation of a Traditional Danish Farmer House. *Build. Environ.* **2022**, *219*, 109174. [CrossRef]
25. Roman, O.; Farella, E.M.; Rigon, S.; Remondino, F.; Ricciuti, S.; Viesi, D. From 3D Surveying Data to Bim to Bem: The Incube Dataset. *Int. Arch. Photogramm. Remote Sens. Spat. Inf. Sci.* **2023**, *XLVIII-1-W3-2023*, 175–182. [CrossRef]

26. Andreucci, M.B. Linking Future Energy Systems with Heritage Requalification in Smart Cities. On-Going Research and Experimentation in the City of Trento (IT). *TECHNE—J. Technol. Archit. Environ.* **2018**, *1*, 87–91. [CrossRef]
27. Fabbri, K.; Zuppiroli, M.; Ambrogio, K. Heritage Buildings and Energy Performance: Mapping with GIS Tools. *Energy Build.* **2012**, *48*, 137–145. [CrossRef]
28. Modelica. Available online: <https://modelica.org/> (accessed on 1 December 2023).
29. Dymola. Available online: <https://www.3ds.com/products/catia/dymola> (accessed on 1 December 2023).
30. Lucchi, E. Renewable Energies and Architectural Heritage: Advanced Solutions and Future Perspectives. *Buildings* **2023**, *13*, 631. [CrossRef]
31. Greek Technical Chamber. TOTEE 20701-1 Technical Guidelines on Buildings' Energy Performance 2017. Greek Technical Chamber: Athens, Greece, 2017.
32. Thomas, D.; Bagheri, A.; Feldheim, V.; Deblecker, O.; Ioakimidis, C.S. Energy and Thermal Comfort Management in a Smart Building Facilitating a Microgrid Optimization. In Proceedings of the IECON 2017—43rd Annual Conference of the IEEE Industrial Electronics Society, Beijing, China, 29 October–1 November 2017; pp. 3621–3626.
33. Bellos, E.; Iliadis, P.; Papalexis, C.; Rotas, R.; Mamounakis, I.; Sougkakis, V.; Nikolopoulos, N.; Kosmatopoulos, E. Holistic Renovation of a Multi-Family Building in Greece Based on Dynamic Simulation Analysis. *J. Clean. Prod.* **2022**, *381*, 135202. [CrossRef]
34. Arandelovic, B.; Musil, R. The Renovation, Rehabilitation and Adaptation of Historical Heritage Buildings in Public Ownership. The Case of Historical Buildings of Exceptional Importance in Vienna. *Build. Environ.* **2023**, *246*, 110937. [CrossRef]
35. Masullo, M.; Pellegrino, R.; Scorpio, M.; Maffei, L. Auditory and Visual Impact of Split Systems on the Façade of Historical Buildings. *Appl. Acoust.* **2021**, *178*, 107997. [CrossRef]
36. newwave-media.it, N. srl- GSP Pompe di calore geotermiche polivalenti. Eneren. Available online: <https://eneren.it/prodotti/gsp/> (accessed on 11 January 2024).
37. Viesi, D.; Galgaro, A.; Visintainer, P.; Crema, L. GIS-Supported Evaluation and Mapping of the Geo-Exchange Potential for Vertical Closed-Loop Systems in an Alpine Valley, the Case Study of Adige Valley (Italy). *Geothermics* **2018**, *71*, 70–87. [CrossRef]
38. Viesi, D.; Mahbub, M.S.; Brandi, A.; Thellufsen, J.Z.; Østergaard, P.A.; Lund, H.; Baratieri, M.; Crema, L. Multi-Objective Optimization of an Energy Community: An Integrated and Dynamic Approach for Full Decarbonisation in the European Alps. *Int. J. Sustain. Energy Plan. Manag.* **2023**, *38*, 8–29. [CrossRef]
39. Tegola Canadese. Available online: <https://www.aleo-solar.de/en> (accessed on 10 January 2024).
40. Technical Guidelines of Technical Chamber of Greece; TEE: Athens, Greece, 2020.
41. ISO 6946:2017; Building Components and Building Elements—Thermal Resistance and Thermal Transmittance—Calculation Methods. ISO: Geneva, Switzerland, 2017. Available online: <https://www.iso.org/standard/65708.html> (accessed on 9 January 2024).
42. Kitsopoulou, A.; Zacharis, A.; Ziozas, N.; Bellos, E.; Iliadis, P.; Lampropoulos, I.; Chatzigeorgiou, E.; Angelakoglou, K.; Nikolopoulos, N. Dynamic Energy Analysis of Different Heat Pump Heating Systems Exploiting Renewable Energy Sources. *Sustainability* **2023**, *15*, 11054. [CrossRef]
43. Duffie, J.; Beckman, W.; Blair, N. Design of Photovoltaic Systems. In *Solar Engineering of Thermal Processes, Photovoltaics and Wind*; John Wiley & Sons, Ltd.: Hoboken, NJ, USA, 2020; pp. 760–788. ISBN 978-1-119-54032-8.
44. Maoucha, A.; Djeffal, F.; Arar, D.; Lakhdar, N.; Bendib, T.; Abdi, M.A. An Accurate Organic Solar Cell Parameters Extraction Approach Based on the Illuminated I-V Characteristics for Double Diode Modeling. In Proceedings of the 2012 First International Conference on Renewable Energies and Vehicular Technology, Nabeul, Tunisia, 26–28 March 2012; pp. 74–77.
45. Hairer, E.; Norsett, S.P.; Wanner, G. *Solving Ordinary Differential Equations I*; Springer Series in Computational Mathematics; Springer: Berlin/Heidelberg, Germany, 1993; Volume 8, ISBN 978-3-540-56670-0.
46. Bellos, E.; Iliadis, P.; Papalexis, C.; Rotas, R.; Nikolopoulos, N.; Kosmatopoulos, E.; Halmdienst, C. Dynamic Investigation of Centralized and Decentralized Storage Systems for a District Heating Network. *J. Energy Storag.* **2022**, *56*, 106072. [CrossRef]
47. EN 15265:2007; Energy Performance of Buildings—Calculation of Energy Needs for Space Heating and Cooling Using Dynamic Methods—General Criteria and Validation Procedures. European Standards: Brussels, Belgium, 2007. Available online: <https://standards.iteh.ai/catalog/standards/cen/3b7d56e1-21c8-4f7f-8fe0-eb9a39c80893/en-15265-2007> (accessed on 13 December 2023).
48. Balaras, C.A.; Dascalaki, E.G.; Psarra, I.; Cholewa, T. Primary Energy Factors for Electricity Production in Europe. *Energies* **2023**, *16*, 93. [CrossRef]
49. Senior, C.; Salaj, A.T.; Vukmirovic, M.; Jowkar, M.; Kristl, Ž. The Spirit of Time—The Art of Self-Renovation to Improve Indoor Environment in Cultural Heritage Buildings. *Energies* **2021**, *14*, 4056. [CrossRef]
50. Integrated National Energy and Climate Plan. | UNEP Law and Environment Assistance Platform. Available online: <https://leap.unep.org/en/countries/it/national-legislation/integrated-national-energy-and-climate-plan> (accessed on 5 March 2024).

51. Ministry of the Environment and Energy Security, Italian National Integrated Plan for Energy and Climate—June 2023. Available online: [https://commission.europa.eu/system/files/2023-07/ITALY%20-%20DRAFT%20UPDATED%20NECP%202021%20030%20\(1\).pdf](https://commission.europa.eu/system/files/2023-07/ITALY%20-%20DRAFT%20UPDATED%20NECP%202021%20030%20(1).pdf) (accessed on 5 March 2024).
52. Anelli, D.; Tajani, F. Valorization of Cultural Heritage and Land Take Reduction: An Urban Compensation Model for the Replacement of Unsuitable Buildings in an Italian UNESCO Site. *J. Cult. Herit.* **2022**, *57*, 165–172. [CrossRef]

Disclaimer/Publisher's Note: The statements, opinions and data contained in all publications are solely those of the individual author(s) and contributor(s) and not of MDPI and/or the editor(s). MDPI and/or the editor(s) disclaim responsibility for any injury to people or property resulting from any ideas, methods, instructions or products referred to in the content.